ISSN: 1992-8645 www.jatit.org E-ISSN: 1817-3195

NARX-BASED VIRTUAL IMU SENSOR FOR FAULT-TOLERANT ATTITUDE ESTIMATION AND CONTROL OF QUADROTOR UAVS

BUI THANH TUNG[1], TRAN THI VAN[2], NGUYEN VAN THANG[3], KHOA NGUYEN DANG[4*]

[1]Faculty of Engineering and Technology, International School, Vietnam National University, Hanoi, Vietnam
[2]Faculty of Information Technology, University of Labour and Social Affairs, Hanoi, Vietnam
[3]University of Engineering and Technology, Vietnam National University, Hanoi, Vietnam
[4]Faculty of Engineering and Technology, International School, Vietnam National University, Hanoi, Vietnam
E-mail: [1]buithanhtung@vnu.edu.vn, [2]vantt@ulsa.edu.vn, [3]nvthangdtvt@vnu.edu.vn, [4]khoand@vnuis.edu.vn

ABSTRACT

Accurate attitude estimation is a fundamental requirement for achieving stable flight and reliable control of quadrotor unmanned aerial vehicles (UAVs). However, failures or abnormal measurements of the Inertial Measurement Unit (IMU) may interrupt attitude feedback and severely degrade flight performance. This paper proposes a Virtual IMU Sensor (VIMUS) based on a Nonlinear AutoRegressive network with eXogenous inputs (NARX) to estimate roll and pitch angles from control inputs and quadrotor dynamics. To evaluate its effectiveness, a Multilayer Perceptron (MLP)-based virtual sensor is implemented as a benchmark under identical training conditions. An IMU fault detection and switching mechanism is further integrated to automatically replace the original IMU with the proposed VIMUS when sensor faults occur. Simulation results show that the NARX-based VIMUS outperforms the MLP model, reducing the root mean square error (RMSE) by 62.3% and 64.6% for roll and pitch estimation, respectively, while achieving coefficients of determination (R^2) of 0.986 and 0.991. The proposed framework enables continuous attitude feedback and provides an accurate and robust fault-tolerant solution for quadrotor attitude estimation and control.

Keywords: *NARX Neural Network, Multilayer Perceptron, IMU Fault Detection, Quadrotor UAV, Attitude Estimation*

1. INTRODUCTION

Unmanned aerial vehicles (UAVs), especially quadrotors, are becoming extremely relevant in both civilian and military applications because of their high maneuverability, ability to perform vertical take-off and landing, and simple mechanical construction. These UAVs have found application in precision agriculture, infrastructure inspection, environment monitoring, emergency relief, aerial mapping, and various surveillance tasks [1-4]. Most of these applications need autonomous operation in dynamic and complicated environment, where a good flight control is required in order to ensure that the mission will be accomplished successfully. Therefore, the attitude estimation becomes one of the most important parts of a quadrotor control system.

As for quadrotor UAVs, the translational movement is performed indirectly with help of the attitude control and thus roll and pitch angles are vital for trajectory tracking and stabilization [5-7]. The information on these attitude states is usually provided by an Inertial Measurement Unit (IMU), consisting of accelerometers and gyros, which provides the orientation estimation. Modern IMUs give very high-frequency measurements, however, they are subjected to such problems as measurement noise, bias drift, vibrations, and various external influences. Even more importantly, IMU failures, communication faults, or abnormal sensor output might break the attitude feedback loop.

In order to enhance estimation accuracy, many sensor fusion algorithms based on IMU data with GPS, magnetometer, vision sensors, or other sensors mounted on board have been presented [8-11].

Traditional approaches such as Extended Kalman Filter (EKF), Unscented Kalman Filter (UKF), and complementary filter can achieve good results under typical situations. However, the aforementioned algorithms usually rely on the availability of IMU measurements. Once serious faults happen in sensors or IMU system malfunctions happen, the estimation capability may be seriously affected, and thus, the reliability of the whole flight control system would be decreased.

Fault-tolerance technology has become a hot topic in order to make UAVs more reliable. FDIs, observer-based methods, Unknown Input Observer (UIO), and Analytical Redundancy approaches are representative [12-14]. They are capable of detecting abnormal sensor behaviors and finding out the faulty parts. However, current methods mainly concentrate on fault detection but not on fault accommodation. Once faults are detected, they often use redundant sensors or precise mathematical model to estimate the states of the system. These kinds of methods add extra cost to the system and limit its applicability to lightweight quadrotor UAVs.

New developments in AI research have presented data-based methods for modeling nonlinear systems and state estimation. Neural networks have shown great potential for modeling complex nonlinear dynamics without any need for exact mathematical formulations [15-19]. In particular, the Nonlinear AutoRegressive with eXogenous inputs (NARX) has received special attention due to the ability to include delayed inputs and delayed outputs in the learning phase of the neural network so that it can model the temporal dynamics of dynamic systems. Due to this nature, NARX neural networks have been successfully used in system identification, prediction of trajectories, modeling of flight dynamics, and attitude estimation of UAVs [25-32]. As compared with traditional feedforward neural networks like the Multilayer Perceptron (MLP), the NARX network contains some memory in its structure which may make it a better candidate for the modeling of the quadrotor dynamics.

Inspired by the aforementioned observations, this work designs a NARX-based Virtual IMU Sensor (VIMUS) to implement fault-tolerant attitude estimation and control of quadrotor UAVs. This virtual sensor models the nonlinear mapping between the control inputs of quadrotor and its attitude response to predict roll and pitch angles independently of physical IMU sensor data. To objectively evaluate the performance of the designed virtual sensor, an MLP-based virtual sensor is designed using the same datasets, architecture settings, and training schemes. Furthermore, an IMU fault detector and auto-switching technique is incorporated into the control system to automatically switch from the actual IMU to the VIMUS when the IMU faults occur. Thus, the attitude feedback will not be interrupted.

The main contributions of this paper are summarized as follows:

(1) A NARX-based Virtual IMU Sensor is developed to reconstruct quadrotor roll and pitch angles from control inputs and system dynamics without relying on physical IMU measurements.

(2) A comprehensive comparative evaluation between NARX and MLP networks is conducted under identical training and testing conditions to investigate the benefits of temporal memory in virtual attitude estimation.

(3) A fault-tolerant framework integrating IMU fault detection and automatic sensor switching is proposed to maintain continuous attitude feedback during sensor failures.

(4) Extensive MATLAB/Simulink simulations demonstrate that the proposed framework significantly improves estimation accuracy and preserves stable attitude control under IMU fault scenarios.

The remainder of this paper is organized as follows. Section 2 presents the mathematical model of the quadrotor UAV. Section 3 describes the PID-based attitude control system. Section 4 introduces the proposed virtual IMU sensor and the benchmark MLP model. Section 5 discusses the simulation setup and experimental results. Finally, Section 6 concludes the paper.

2. QUADROTOR SYSTEM MODELING

In this paper, a plus-type quadrotor configuration is considered to develop the proposed control algorithm. The system consists of four rotors driven by four independent motors, as shown in Fig. 1. Motors (1, 3) rotate in the same direction, while motors (2, 4) rotate in the opposite direction to generate balanced thrust and ensure stable flight.

Let the coordinate frames $OXYZ$ and $OX_eY_eZ_e$ represent the body-fixed frame B and the inertial frame E, respectively. The state variables $(X, Y, Z, \phi, \theta, \psi)$ describe the position and Euler angles of the quadrotor. In particular, roll (ϕ), pitch (θ), and yaw (ψ) represent rotations about the X, Y, and Z axes of the body frame, respectively.

Journal of Theoretical and Applied Information Technology
31st August 2026. Vol.104. No.16

ISSN: 1992-8645 www.jatit.org E-ISSN: 1817-3195

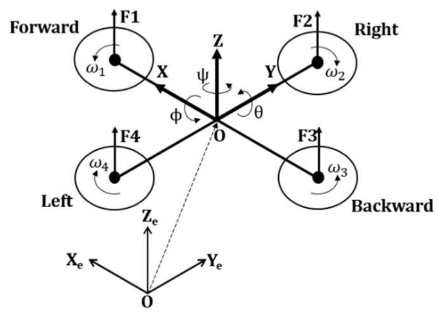

Figure 1: The Geometry Of Quadrotor Typed Plus

The control inputs (U_1, U_2, U_3, U_4) correspond to the thrust and moments acting on the quadrotor, governing the motion along Z and the rotational dynamics (ϕ, θ, ψ), respectively [30, 33]

$$U_1 = b\left(\omega_1^2 + \omega_2^2 + \omega_3^2 + \omega_4^2\right) \quad (1)$$

$$U_2 = b\left(\omega_4^2 - \omega_2^2\right) \quad (2)$$

$$U_3 = b\left(\omega_1^2 - \omega_3^2\right) \quad (3)$$

$$U_4 = d\left(\omega_1^2 - \omega_2^2 + \omega_3^2 - \omega_4^2\right) \quad (4)$$

Where ω_i denotes the rotor angular velocity $(i = 1..4)$. The parameters b and d represent the thrust coefficient and the drag coefficient, respectively. The translational and rotational dynamics of the quadrotor are described in Eq. (5) and Eq. (6) [30, 34]. The system parameters are summarized in Table 1.

$$\begin{bmatrix} \ddot{X} \\ \ddot{Y} \\ \ddot{Z} \end{bmatrix} = \begin{bmatrix} (\cos\phi \sin\theta \cos\psi + \sin\phi \sin\psi)\dfrac{U_1}{m} \\ (\cos\phi \sin\theta \sin\psi - \sin\phi \cos\psi)\dfrac{U_1}{m} \\ (\cos\phi \cos\theta)\dfrac{U_1}{m} - g \end{bmatrix} \quad (5)$$

$$\begin{bmatrix} \ddot{\phi} \\ \ddot{\theta} \\ \ddot{\psi} \end{bmatrix} = \begin{bmatrix} \dfrac{(I_y - I_z)}{I_x}\dot{\theta}\dot{\psi} - \dfrac{J_r}{I_x}\dot{\theta}\Omega_r + \dfrac{U_2 l}{I_x} \\ \dfrac{(I_z - I_x)}{I_y}\dot{\phi}\dot{\psi} + \dfrac{J_r}{I_y}\dot{\phi}\Omega_r + \dfrac{U_3 l}{I_y} \\ \dfrac{(I_x - I_y)}{I_z}\dot{\phi}\dot{\theta} + \dfrac{U_4}{I_z} \end{bmatrix} \quad (6)$$

where $\Omega_r = \omega_1 - \omega_2 + \omega_3 - \omega_4$ and the parameters are shown in Table. 1.

Table 1: Parameters Of Rotational And Translational Dynamics Equations

Symbol	Meaning	Unit
m	Mass of Quadrotor	Kg
I_x , I_y ,I_z	Inertia constants	Kg.m^2
J_r	Rotor inertia	Kg.m2
l	Arm length	m
g	Gravitation	m/s^2

The mathematical model presented in this section is used to generate state trajectories for neural network training and validation. In particular, roll and pitch responses, together with the corresponding control inputs, are collected from the closed-loop system and used to construct datasets for both the proposed NARX-based VIMUS and the benchmark MLP model. This ensures a consistent and fair comparison between the two neural network architectures under identical dynamic conditions.

3. CONTROLLER DESIGN OF QUADROTOR UAV

Normally, UAV design control contains two loops in Fig. 2: the position control and the attitude control. The outer loop is used to control the quadrotor followed the desired trajectory (X_d, Y_d, Z_d), and the inner loop is used to control the quadrotor to achieve the desired attitude $(\phi_d, \theta_d, \psi_d)$.

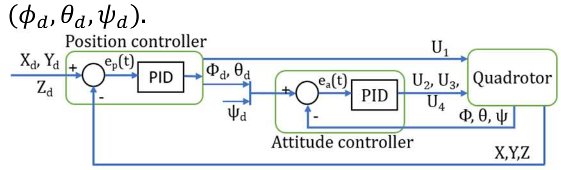

Figure 2: UAV Quadrotor Controller

In this paper, the proportional integral derivative (PID) controller is developed in both the position and attitude controller to drive all operators of the UAV quadrotor. The output of each controller is presented in PID form as:

$$U(t) = K_p(e(t)) + K_i\int(e(t))dt + K_d d\frac{(e(t))}{dt} \quad (7)$$

Where the K_p, K_i, K_d parameters are the gains of the PID controllers and $e(t)$ presents for the error control.

From Fig. 2, the attitude controller needs to be feedbacked on the roll and pitch from the UAV which can be measured from the IMU sensor. This task is very important for quadrotor controllers. However, the usage of IMU sensors requires a lot of calculation and needs to combine additional filters to

ISSN: 1992-8645 www.jatit.org E-ISSN: 1817-3195

achieve a better result [35]. In addition, the IMU could be broken and gain larger errors. Therefore, we propose a new method to replace the IMU sensor with a virtual sensor based on the NARX network which is capable of solving the complex nonlinear dynamics as a quadrotor.

In the proposed control architecture, the attitude controller relies on roll and pitch feedback signals to stabilize the quadrotor dynamics. Under normal conditions, these signals are provided by the OIMU. However, in the presence of sensor faults or abnormal disturbances, the proposed VIMUS is used as a substitute to provide estimated attitude feedback. This integration ensures that the PID-based attitude control loop remains operational even when the physical IMU becomes unreliable or fails.

4. VIRTUAL IMU SENSOR DEVELOPMENT AND COMPARATIVE NEURAL NETWORK MODELING

In this section, a VIMUS based on a NARX is developed to estimate quadrotor attitude states in real time. The proposed model is designed to reconstruct roll and pitch angles using control input signals and past output states, eliminating the dependence on physical IMU measurements.

4.1 NARX-based Virtual IMU Model

The NARX network is formulated as a dynamic recurrent model with delayed inputs and outputs. The input vector consists of current and past control signals (U2, U3) and previous attitude states (ϕ, θ), while the output corresponds to the estimated roll and pitch angles.

The inclusion of time-delay terms enables the model to capture the temporal evolution of quadrotor dynamics, which is essential for accurate attitude estimation in nonlinear systems.

The roll and pitch dynamics are expressed in discrete-time form as:

$$\left[\phi(t),\theta(t)\right]=f\begin{bmatrix}\phi(t-1),\theta(t-1),\phi(t-2),\theta(t-2)\\ ,U_2(t),U_3(t),U_2(t-1),U_3(t-1)\\ ,U_2(t-2),U_3(t-2)\end{bmatrix} \quad (8)$$

Where $\phi(t)$ and $\theta(t)$ denote the estimated roll and pitch angles at time t. The term $\phi(t-1),\phi(t-2),\theta(t-1)$, $\theta(t-2)$ represent past attitude states, while $U_2(t)$, $U_3(t)$ and their delayed values represent control inputs affecting the system dynamics.

Based on Eq. (8), the VIMUS architecture is constructed as shown in Fig. 3, consisting of an input layer, a hidden layer with H neurons, and an output layer with two neurons corresponding to roll and pitch estimation.

4.2 NARX-based Virtual IMU Model

To evaluate the effectiveness of the proposed approach, a conventional MLP network is implemented as a benchmark model.

The MLP consists of an input layer, two hidden layers with nonlinear activation functions, and an output layer. The network uses the same input and output variables as the NARX model but does not include time-delay feedback connections, representing a static nonlinear mapping.

Both NARX and MLP models are trained using identical datasets, preprocessing procedures, and data partitioning (training, validation, and testing sets) to ensure a fair comparison under consistent conditions.

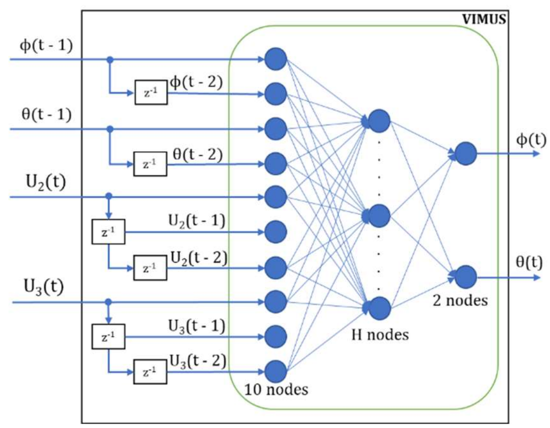

Figure 3: Design Of VIMUS For Predicting The Roll And Pitch Of Quadrotor

4.3 Training Procedure

The datasets used for training are obtained from the closed-loop quadrotor simulation described in Section 2. All input and output signals are normalized prior to training to improve numerical stability and convergence performance.

Fig. 4 illustrates the integrated training framework of the proposed VIMUS within the quadrotor closed-loop system. The neural network is trained using input-output data generated from the UAV dynamics model, enabling supervised learning of the nonlinear attitude mapping.

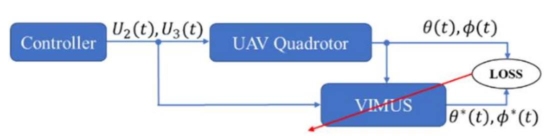

Figure 4: Integrated VIMUS To UAV Quadrotor For Training Process

Journal of Theoretical and Applied Information Technology
31st August 2026. Vol.104. No.16

ISSN: 1992-8645 www.jatit.org E-ISSN: 1817-3195

The NARX network is configured with 10 hidden neurons and two-time-step delays. The learning process uses backpropagation [36] with mean squared error (MSE) [37] as the loss function. Early stopping based on validation error is applied to avoid overfitting.

For consistency, the MLP model is trained using the same dataset, normalization procedure, and training strategy as the NARX model.

The VIMUS parameters are updated iteratively using gradient-based backpropagation as:

$$E(t)=\frac{1}{2}\left[\left(\phi(t)-\phi^{*}(t)\right)^{2}+\left(\theta(t)-\theta^{*}(t)\right)^{2}\right] \tag{9}$$

$$p_i(t+1)=p_i(t)-\mu*\frac{\partial E(t)}{\partial p_i(t)} \tag{10}$$

Where μ is the learning rate, and $p_i(t)$ representsthe weight of the i^{th} neurons at time t.

In this formulation, $\emptyset^*(t)$ and $\theta^*(t)$ denote the reference roll and pitch angles generated from the quadrotor simulation model. These values are used as target outputs for supervised learning to train the VIMUS network. The predicted outputs of the neural network are denoted as $\emptyset(t)$ and $\theta(t)$, which are compared against the reference values during the training process.

The training performance is evaluated using the MSE criterion. As shown in Fig. 5, the network converges after approximately 1000 iterations with a final MSE of 1.8361×10^{-8}, indicating stable learning behavior.

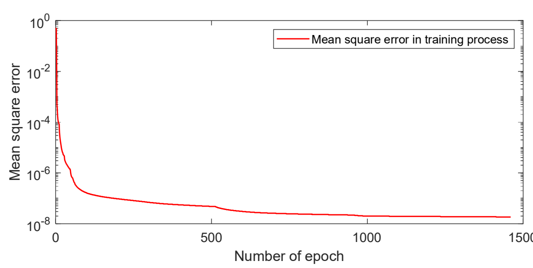

Figure 5: Training Performance Of VIMUS

4.4 Fault Detection and Switching Strategy

To ensure fault-tolerant operation, a switching mechanism is designed to select between the OIMU and the proposed VIMUS.

The switching decision is based on the estimation error between the measured IMU signals and the virtual sensor outputs, defined as:

$$\mathrm{e}(t) = \|x_{IMU}(t) - x_{VIMUS}(t)\| \tag{11}$$

where $x_{IMU}(t)$ represents the measured attitude from the physical IMU and $x_{VIMUS}(t)$ represents the estimated attitude from the proposed model.

When the error $\mathrm{e}(t)$ exceeds a predefined threshold ε, the system automatically switches from OIMU to VIMUS to maintain reliable attitude feedback for the controller.

This hybrid architecture ensures continuous availability of attitude information and enhances the fault-tolerant capability of the quadrotor UAV under sensor degradation or failure conditions.

The overall integration of the proposed VIMUS into the quadrotor closed-loop control system for testing and validation purposes is illustrated in Fig. 6. In this configuration, the VIMUS operates as an alternative feedback source to OIMU when sensor anomalies are detected, ensuring continuous attitude estimation for the controller.

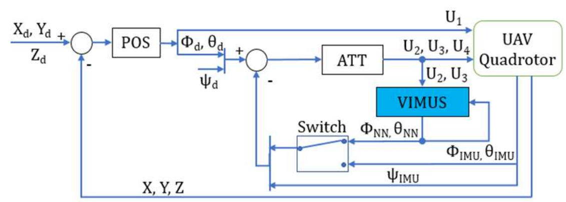

Figure 6: Integrated VIMUS To UAV Quadrotor For The Testing Process

When the deviation exceeds a predefined threshold, the system automatically switches to VIMUS to maintain stable attitude feedback for the controller.

This hybrid architecture ensures continuous availability of attitude information even under sensor degradation or failure conditions.

The same training configuration is applied to both NARX and MLP models to ensure a fair comparison.

To further evaluate the prediction capability of the proposed VIMUS, a conventional MLP neural network with the same training dataset was implemented as a benchmark model. The performance of both models was assessed using RMSE, MAE, and R^2 metrics. Furthermore, the prediction errors of roll and pitch angles were compared to demonstrate the effectiveness of the NARX architecture in capturing the temporal dynamics of quadrotor attitude motions.

5. SIMULATION AND RESULTS

In this section, the performance of the proposed VIMUS is evaluated through comprehensive MATLAB/Simulink simulations. The quadrotor UAV model, including its physical

Journal of Theoretical and Applied Information Technology
31st August 2026. Vol.104. No.16

ISSN: 1992-8645 www.jatit.org E-ISSN: 1817-3195

parameters and control gains, is summarized in Table 3, while the dynamic model parameters are provided in Table 2 [38]. The simulations are conducted over a 30 [s] time horizon to evaluate both trajectory tracking and fault-tolerant capability.

Table 2: Quadrotor Parameters

Symbol	Value	Unit
m	0.650	Kg
I_x	7.5×10^{-3}	Kg.m2
I_y	7.5×10^{-3}	Kg.m^2
I_z	1.3×10^{-2}	Kg.m^2
I_r	6×10^{-5}	Kg.m^2
d	7.5×10^{-7}	N.m.s^2
b	3.13×10^{-5}	N.s^2
l	0.23	m
g	9.81	m/s^2

Table 3: Gain Of PID Controller

PID gains	Position Controller			Attitude Controller		
	X	Y	Z	ϕ	θ	ψ
K_p	5	5	70	5	5	5
K_i	0	0	20	0	0	0
K_d	4	4	20	0.4	0.4	0.4

5.1 Baseline Quadrotor Performance

Initially, the quadrotor system is tested using the conventional PID-based control structure with the OIMU providing roll and pitch feedback. The UAV is commanded to follow a time-varying trajectory in the $X - Y - Z$ space.

As shown in Fig. 7, the quadrotor successfully tracks the desired trajectory defined as

$X_d = -0.5, -0.43, -0.5, -1.05, -0.17\ (m)$

$Y_d = 0.27, -0.37, -0.54, -0.08, 0.62, 0.82\ (m)$

$Z_d = 1\ (m)$

The results indicate that the PID-based controller ensures stable tracking performance with small steady-state error. The roll and pitch responses also follow their reference signals with slight delays due to the cascaded position-attitude control structure.

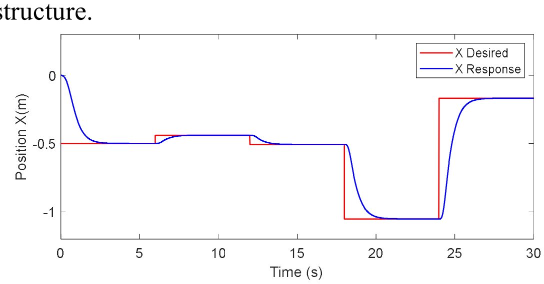

(a) X Position Of UAV Quadrotor

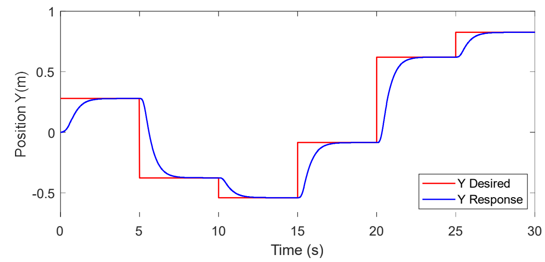

(b) Y Position Of UAV Quadrotor

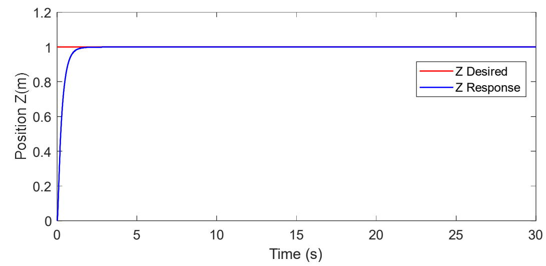

(c) Z Position Of UAV Quadrotor

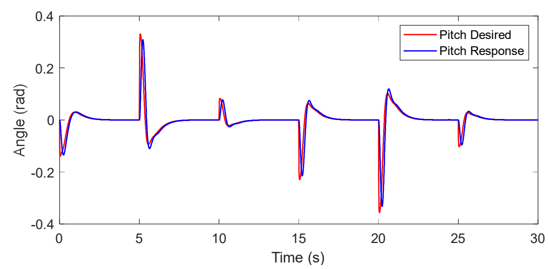

(d) Pitch Of UAV Quadrotor

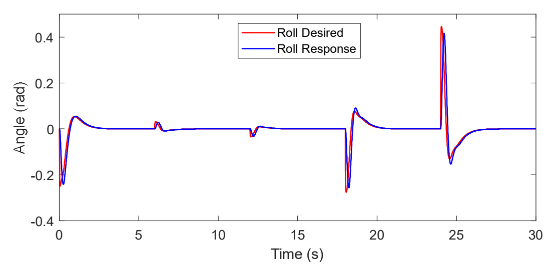

(e) Roll Of UAV Quadrotor

Figure 7: Performance Of Position And Attitude Controller For The Quadrotor

5.2 Performance of VIMUS under Nominal Conditions

To evaluate the effectiveness of the proposed virtual sensing approach under normal operating conditions, the VIMUS is integrated into the quadrotor closed-loop control system, replacing the OIMU for attitude feedback.

As illustrated in Fig. 8, the quadrotor maintains stable trajectory tracking performance when using the proposed VIMUS. The estimated roll and pitch signals generated by the neural network closely follow the expected attitude behavior of the system, indicating that the virtual sensor can

Journal of Theoretical and Applied Information Technology
31st August 2026. Vol.104. No.16

ISSN: 1992-8645 www.jatit.org E-ISSN: 1817-3195

effectively reproduce IMU-like measurements in nominal conditions.

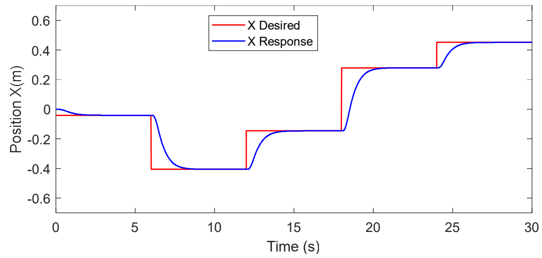

(a) X Position Of UAV Quadrotor

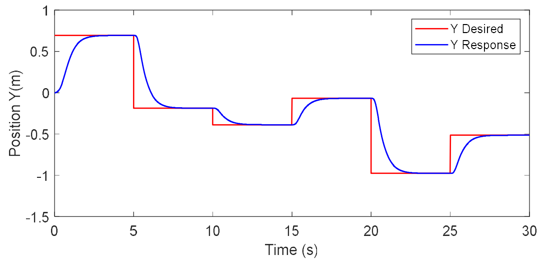

(b) Y Position Of UAV Quadrotor

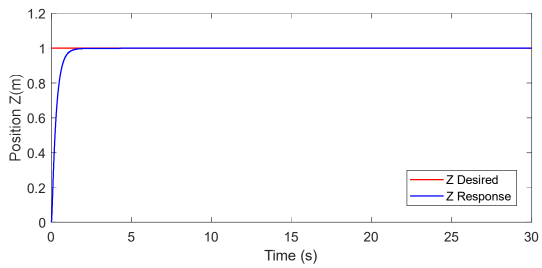

(c) Z position Of UAV Quadrotor

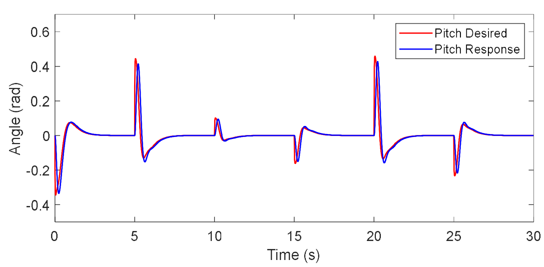

(d) Pitch Of UAV Quadrotor

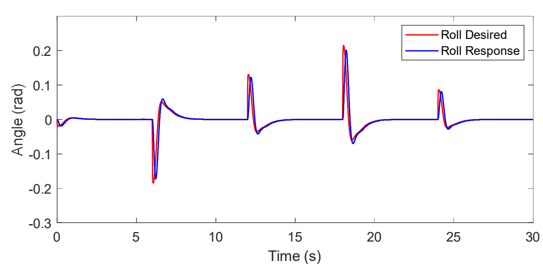

(e) Roll Of UAV Quadrotor

Figure 8: Position And Altitude Angle Of The Quadrotor With Virtual IMU

From a quantitative perspective, the estimation error between the VIMUS outputs and the reference IMU signals remains small and bounded throughout the simulation. This indicates that no significant drift or instability is introduced by the neural network-based estimator during normal flight operation.

In particular, the attitude tracking performance remains consistent with the baseline PID-controlled system, with only minor deviations observed due to neural network approximation effects. These deviations do not affect the overall stability of the quadrotor, confirming that the proposed VIMUS can reliably replace the physical IMU under nominal conditions without degrading control performance.

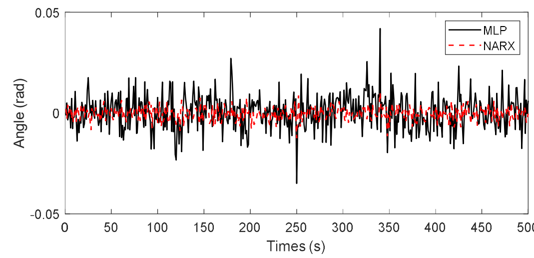

(a) Prediction Error Of Roll

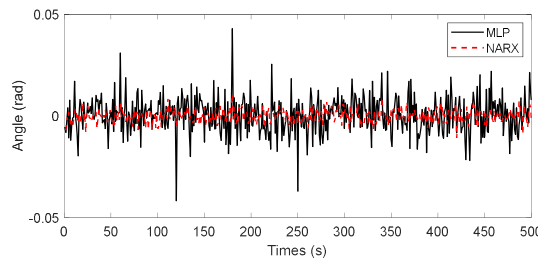

(b) Prediction Error Of Pitch

Figure 9: Prediction Error Comparison Between MLP And NARX

5.3 Comparative Analysis: NARX vs MLP

To validate the effectiveness of the proposed NARX-based architecture, a conventional MLP is implemented as a benchmark model using the same dataset, preprocessing steps, and training configuration. The prediction error comparison is shown in Fig. 9, where the roll and pitch estimation errors are defined as:

$$e_{\emptyset} = \emptyset - \hat{\emptyset} \tag{12}$$

$$e_{\theta} = \theta - \hat{\theta}$$

It is observed that the NARX model significantly reduces prediction errors compared to the MLP model for both attitude variables. This improvement is attributed to the ability of the NARX

Journal of Theoretical and Applied Information Technology
31st August 2026. Vol.104. No.16

ISSN: 1992-8645 www.jatit.org E-ISSN: 1817-3195

network to capture temporal dependencies through delayed inputs and outputs.

As shown in Fig. 9, the NARX model consistently exhibits lower prediction errors compared to the MLP for both roll and pitch estimation. This improvement is mainly due to the recurrent structure of NARX, which incorporates delayed inputs and outputs, enabling it to capture the temporal dependencies and nonlinear dynamics of quadrotor attitude motion more effectively than the static feedforward MLP.

Table 4: Performance Comparison For Roll Angle Estimation

Model	RMSE	MAE	R^2
MLP	0.0085761	0.0067034	0.90165
NARX	0.0032318	0.0025837	0.98603
Error Reduction (%)	62.317	61.457	-
R^2 Gain (%)	-		9.3589

Table 5: Performance Comparison For Pitch Angle Estimation

Model	RMSE	MAE	R^2
MLP	0.008827	0.0067234	0.92806
NARX	0.0031229	0.0024583	0.991
Error Reduction (%)	64.621	63.438	-
R^2 Gain (%)	--	-	6.7812

The quantitative evaluation is further summarized in Tables 4 and 5. It can be observed that the proposed NARX model achieves a significant reduction in prediction error, with more than 60% improvement in both RMSE and MAE for roll and pitch. In addition, the coefficient of determination is substantially improved, reaching R2=0.986 for roll and R2=0.991 for pitch, compared to the MLP results of 0.90165 and 0.92806, respectively.

These results confirm that the proposed NARX-based VIMUS provides a more accurate and reliable attitude estimation compared to the conventional MLP model, making it more suitable for real-time virtual sensing in quadrotor UAV applications.

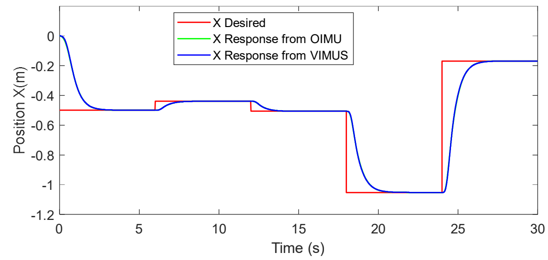

(a) X Position Of UAV Quadrotor

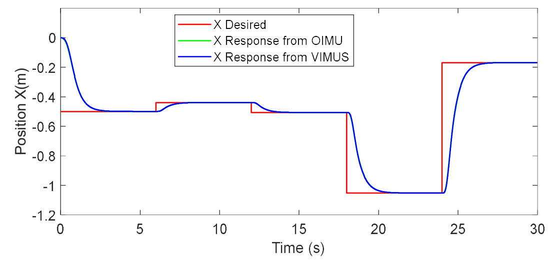

(b) Y Position Of UAV Quadrotor

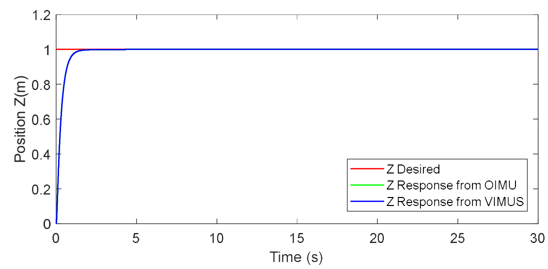

(c) Z Position Of UAV Quadrotor

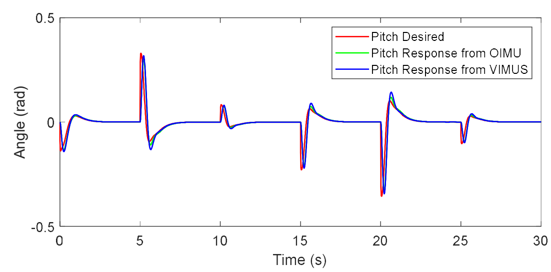

(d) Pitch Of UAV Quadrotor

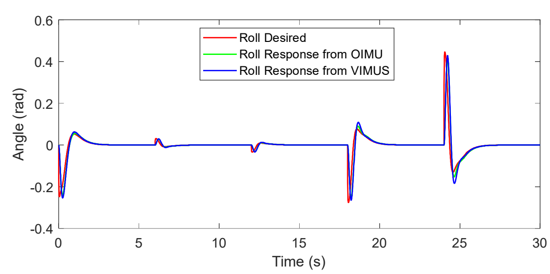

(e) Roll Of UAV Quadrotor

Figure 10: Comparison Between IMU Sensor And Virtual IMU

5.4 Comparative Attitude Performance between OIMU and VIMUS

In this simulation, the quadrotor performance is evaluated under nominal conditions by comparing the OIMU and the proposed VIMUS, as shown in Fig. 10.

As illustrated in Fig. 10(a)-(c), the quadrotor is able to accurately track the desired position trajectories in the X, Y, and Z directions for both OIMU and VIMUS-based configurations. The results indicate that the proposed virtual sensing approach does not degrade the overall position control performance, and both methods ensure stable trajectory tracking under nominal flight conditions.

However, slight differences can be observed in the attitude response, particularly in roll and pitch dynamics. As shown in Fig. 10(d)-(e), the OIMU-based system exhibits lower overshoot compared to the VIMUS at several time instances, including approximately 6 [s], 16 [s], and 21 [s] for pitch response, and 18 [s] and 24 [s] for roll response.

This behavior is mainly attributed to the inherent approximation characteristics and computational delay introduced by the NARX-based virtual sensor. Since the VIMUS requires real-time neural network inference to estimate attitude states, a small latency is introduced in generating roll and pitch outputs. As a result, the VIMUS-based response exhibits slightly higher transient overshoot compared to direct physical IMU measurements.

Despite these minor differences, both approaches demonstrate highly comparable tracking performance in both position and attitude responses. This confirms that the proposed VIMUS can effectively approximate the behavior of a physical IMU while maintaining acceptable control performance under nominal operating conditions.

5.5 Comparative Attitude Performance between OIMU and VIMUS

To further evaluate the robustness of the proposed system, disturbance signals are injected into the OIMU measurements, as illustrated in Fig. 11. Specifically, a pitch disturbance is introduced at t=8 [s], followed by a roll disturbance at t=14 [s]. These perturbations are used to simulate realistic IMU degradation scenarios such as noise spikes, bias drift, and partial sensor malfunction.

As shown in Fig. 11, the injected disturbances significantly corrupt the OIMU measurements. In this case, the measured attitude no longer accurately represents the true system dynamics. As a result, erroneous feedback is propagated to the controller, which leads to degraded tracking performance. In particular, the pitch disturbance directly affects the Y-direction motion, while the roll disturbance introduces additional oscillations in the lateral response.

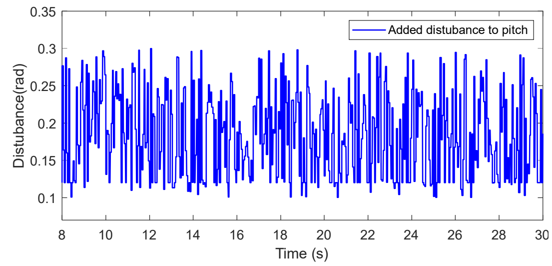

(a) Disturbance Added To Pitch Of UAV Quadrotor

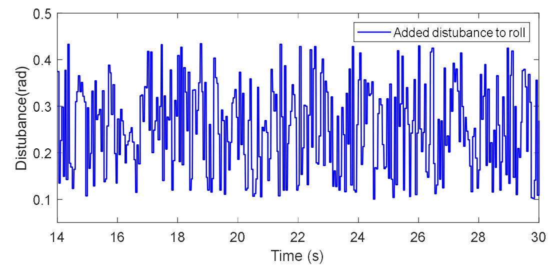

(b) Disturbance Added To Roll Of UAV Quadrotor

Figure 11: Disturbance Added To The Roll And Pitch Of The UAV Quadrotor

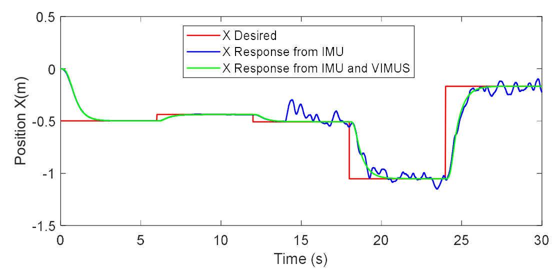

(a) X Position Of UAV Quadrotor

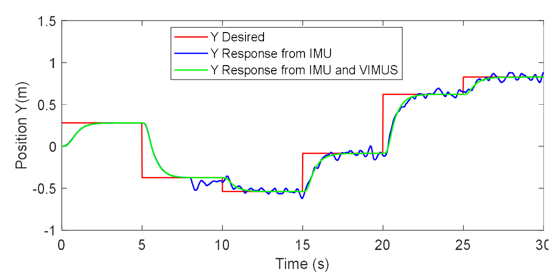

(b) Y Position Of UAV Quadrotor

Figure 12: Replace IMU Sensor With Virtual IMU

To mitigate this issue, the proposed switching mechanism is activated based on the estimation error between the OIMU and the VIMUS. When the error exceeds the predefined threshold ε=0.1, the system automatically switches the feedback source from OIMU to VIMUS.

ISSN: 1992-8645 www.jatit.org E-ISSN: 1817-3195

The resulting system response is shown in Fig. 12. After switching, the quadrotor is able to recover stable trajectory tracking performance despite the presence of IMU disturbances. Although transient deviations are observed immediately after fault injection, the VIMUS-based estimation effectively prevents long-term divergence and restores consistent flight behavior. These results confirm that the proposed architecture significantly improves the robustness of quadrotor UAVs under sensor degradation and partial failure conditions.

6. CONCLUSION

This paper proposed a NARX-based Virtual IMU Sensor for fault-tolerant attitude estimation and control of quadrotor UAVs. The proposed approach models the nonlinear relationship between control inputs and attitude dynamics to estimate roll and pitch angles in real time without relying on physical IMU measurements. A comparative evaluation with a multilayer perceptron showed that the NARX model significantly improves prediction accuracy, achieving more than 60% reduction in RMSE and MAE for both roll and pitch, as well as higher R^2 values exceeding 0.98. In addition, validation against the OIMU demonstrated that the proposed method maintains comparable performance under nominal conditions, with only minor transient differences due to neural network inference delay. Furthermore, under IMU disturbance scenarios, the proposed switching mechanism enables seamless transition to VIMUS, ensuring stable attitude estimation and preserving trajectory tracking performance. These results confirm the effectiveness of the proposed framework for reliable fault-tolerant UAV operation, with future work focusing on real-world implementation and experimental validation.

ACKNOWLEDGEMENT

This research is funded by International School, Vietnam National University, Hanoi (VNU-IS) under project number CS.2025-08.

REFERENCES:

[1]. D. Giordan, et al. (2020). The use of unmanned aerial vehicles (UAVs) for engineering geology applications. Bulletin of Engineering Geology and the Environment, 79(7), 3437-3481.

[2]. P. Garre, and A. Harish. (2018). Autonomous Agricultural Pesticide Spraying UAV. IOP Conference Series: Materials Science and Engineering, 455, 012030.

[3]. A. Utsav, A. Abhishek, P. Suraj, and R. K. Badhai. (2021). An IoT Based UAV Network For Military Applications. IEEE WiSPNET, pp. 122-125.

[4]. M. Gargalakos. (2021). The role of unmanned aerial vehicles in military communications: application scenarios, current trends, and beyond. The Journal of Defense Modeling and Simulation.

[5]. A. L. Salih, M. Moghavvemi, H. A. F. Mohamed, and K. S. Gaeid. (2010). Modelling and PID controller design for a quadrotor UAV. IEEE AQTR, pp. 1-5.

[6]. A. Murilo, and R. V. Lopes. (2019). Unified NMPC framework for VTOL UAV control. Proc. IMechE Part I, 233(7), 889-903.

[7]. W. Alqaisi, et al. (2020). Position and attitude tracking of quadrotor UAVs based on super-twisting algorithm. Proc. IMechE Part I, 234(3), 396-408.

[8]. A. Z. Azfar, and D. Hazry. (2011). IMU sensor fusion for quadrotor stabilization. IEEE ICSPC, pp. 28-32.

[9]. Sumardi, et al. (2019). Inertial Navigation System of Quadrotor Based on IMU and GPS Sensors. ICITACEE, pp. 1-6.

[10]. A. R. Vidal, et al. (2018). Ultimate SLAM: combining events, images, and IMU. IEEE Robotics and Automation Letters, 3, 994-1001.

[11]. G. Loianno, et al. (2017). Aggressive flight control for small quadrotor. IEEE RA-L, 2(2), 404-411.

[12]. Z. Tu, et al. (2018). UAV sensor fault isolation and recovery. arXiv preprint.

[13]. E. D'Amato, et al. (2018). UAV sensor FDI for attitude estimation. IEEE TIM, 67(10), 2465-2475.

[14]. L. Zuo, et al. (2020). Sensor fault diagnosis for quadrotor UAV. CCDC, pp. 4052-4057.

[15]. M. Chen, S. S. Ge, and B. V. E. How. (2010). Adaptive neural network control for nonlinear MIMO systems. IEEE TNN, 21(5), 796-812.

[16]. D. Li, et al. (2019). Neural network control for nonlinear systems. IEEE TNNLS, 30(9), 2625-2636.

[17]. J. Liu, et al. (2023). Neural network learning-based control. IEEE Control Systems Letters, 7, 3579-3584.

[18]. A. Zribi, et al. (2015). PID neural network controller design. arXiv preprint.

[19]. F. Xu, et al. (2014). Adaptive neural network control with U-model. Mathematical Problems in Engineering, 420713.

ISSN: 1992-8645 www.jatit.org E-ISSN: 1817-3195

[20]. R. Kumar, et al. (2019). Neural networks for nonlinear systems identification. Soft Computing, 23(1), 101-114.
[21]. A. Ho Pham Huy, et al. (2008). NARX model for robot arm identification. IEEE ICCE, pp. 18-23.
[22]. H. P. H. Anh, and N. T. Nam. (2012). NARX model for robot arm kinematics. Int. J. Adv. Robot. Syst., 9(4), 104.
[23]. L. Xin, et al. (2020). Mobile robot identification using NARX. Symmetry, 12(9), 1430.
[24]. Y. Yang, and Y. Yan. (2015). Neural sliding mode control for UAV tracking. Proc. IMechE Part I, 229(6), 529-540.
[25]. A. Altan, et al. (2018). NARX-based control for hexarotor UAV. CEIT, pp. 1-6.
[26]. A. Avdeev, et al. (2021). NARX-based quadrotor identification. Applied Artificial Intelligence, 35(4), 265-289.
[27]. M. F. Pairan, et al. (2020). Review of neural network UAV modeling. J. Advanced Mechanical Engineering Applications, 1(2), 20-33.
[28]. M. Collotta, et al. (2014). Neural network real-time control hexacopter. ISPE, pp. 222-227.
[29]. V. Artale, et al. (2016). Neural network PID flight control. Applied Mathematics and Information Sciences, 10, 395-402.
[30]. S. R. C, et al. (2012). Quadrotor UAV design and implementation. Engineering Applications Workshop, pp. 1-6.
[31]. M. Badwan, and T. A. Tutunji. (2018). System identification for Bixler UAV. REM, pp. 93-98.
[32]. M. F. Q. Say, et al. (2019). UAV attitude estimation using ANN. IEEE HNICEM, pp. 1-4.
[33]. G. P. S. Rible, et al. (2020). Propeller parameter modeling for quadrotor. arXiv preprint.
[34]. S. Abdelhay, and A. Zakriti. (2019). PID-based UAV trajectory tracking model. Procedia Manufacturing, 32, 564-571.
[35]. H. Q. T. Ngo, et al. (2017). Complementary vs Kalman filter UAV. IEEE ICSSE, pp. 488-493.
[36]. H. Wang, and G. Song. (2014). NARX model for SMA wire system. Neurocomputing, 134, 289-295.
[37]. M. Saghafi, and M. B. Ghofrani. (2019). LOCA size estimation using NARX NN. Nuclear Engineering and Technology, 51(3), 702-708.
[38]. S. R. Munasinghe. (2025). A Quadrotor Simulation and Research Platform. Drones and Autonomous Vehicles, 2, 10014. https://doi.org/10.70322/dav.2025.10014